Emission stimulation in a directional band gap of a CdTe-loaded opal photonic crystal

S. G. Romanov, D. N. Chigrin, and C. M. Sotomayor Torres
Institute of Materials Science and Department of Electrical and Information Engineering, University of Wuppertal, Gauss-strasse 20, 42097 Wuppertal, Germany

N. Gaponik, A. Eychmüller, and A. L. Rogach
Institute of Physical Chemistry, University of Hamburg, Grindelallee 117, 20146 Hamburg, Germany
(Received 18 June 2003; revised manuscript received 15 January 2004; published 27 April 2004)

An anisotropic photonic crystal light source has been realized by impregnation of a thin film latex opal with brightly luminescent CdTe nanocrystals. Its photoluminescence along a given direction has been studied as a function of excitation power. An increase of the photoluminescence saturation threshold in the directional photonic band gap has been observed. This result is interpreted as a stimulation of emission coupled to specific eigenmodes of a directional band gap. A theoretical model exploiting the low group velocity eigenmodes has been elaborated to explain the resonance character of the emission with band gap frequencies.

DOI: 10.1103/PhysRevE.69.046606 PACS number(s): 42.70.Qs, 78.55.−m

One of the most fascinating issues in the field of photonic crystals (PhCs) is the prospect of improved performance of PhC-embedded light sources [1,2]. In the case of a complete photonic band gap (PBG), the emission enhancement can be achieved due to the abrupt variation of the density of optical modes associated with the PBG edge [3] or the defect state inside the PBG [4]. In the case of a weak dielectric constant modulation, the coherent scattering of electromagnetic (EM) waves leads to lasing at the lattice-constant-related frequency, in particular, it was observed in liquid-infiltrated opals [5]. Both mechanisms exploit the backreaction of the emitted EM radiation on the radiative transition, which makes the emission in such modes a nonlinear process.

Three-dimensional PhCs are required to achieve the full PBG control upon the emission. In the visible, artificial opals have the necessary lattice parameters and offer readily available PhC light sources. The drawback of opals is their poor crystallinity, which results in scrambling of photon trajectories, if the PhC thickness exceeds the photon mean free path (MFP) [6]. In current research-grade opals coherent phenomena degrade with increasing refractive index (RI) contrast due to shorter MFP. Better results are expected for opals prepared as thin films [7], so that the MFP becomes comparable to the film thickness. Correspondingly, the majority of emitted photons can leave the opal without being scattered by defects [8]. This allows the detection of the emission into a given optical mode outside the opal.

Changes of the emission rate in moderate RI contrast opals were studied [9–11], however, the findings remain a matter of discussions due to possible averaging of the emission probability over all realizations of the emitter-mode coupling, when the emitter occupies more than 20% of the unit-cell volume [6,12]. In our work, brightly emitting CdTe nanocrystals (NCs) [13] were attached to the surface of opal spheres. Such configuration avoids the coupling strength averaging, because NCs occupy only a small volume of the unit cell near the dielectric-air boundary [14]. The averaging over randomly oriented dipoles results in an isotropic light source. In this case, the distortion of the spherical wave front of the isotropic light source results only from the anisotropy of the PBG. We will refer to the space fraction shadowed by the first PBG in the wave front as the Bragg cone.

Eigenmodes of lattice defects or modes of low group velocity [15] fill partly the Bragg cone. These modes differ dramatically from the Bloch waves of allowed bands and one can expect a difference in the emission dynamics of dipoles coupled to these specific modes. Here we report the observation of the PBG-related alteration of the radiative relaxation of NCs by examining input-output photoluminescence (PL) characteristics over a frequency interval including PBG and explain our observations using the low group velocity eigenmodes.

Colloidal suspension of latex spheres of $D=240$ nm diameter was dried on glass slides (1 cm^2) to prepare opal films. Films crystallize in the fcc lattice, with the [111] growth direction. Subsequently, films with a thickness of 20–30 μm were sintered for 2 h at 100 °C. CdTe NCs [16] protected by an organic shell to prevent their agglomeration were infiltrated into opal films. As a result of electrical charging of the shells, the CdTe NCs are attached to the surface of latex spheres [Fig. 1(a)].

Transmission spectra of the opal films were measured under white light illumination. The transmitted light was collected within a solid angle $\Omega=2°$. The PL was excited by the 351 nm line of a continuous wave Ar^+ laser, with power up to 6 mW in a 0.1 mm diameter spot, and collected within a $\Omega=5°$ from the film face opposite to that exposed to laser beam [Fig. 1(b)]. PL spectra were measured at three angles θ with respect to the [111] axis of the opal lattice.

To avoid a dramatic change of the emission intensity over wide spectral range, the PL spectrum of the CdTe opal was broadened exploiting the partial degradation of the NC luminescence after intense white light illumination. The PL spectrum of CdTe opal collected at $\theta=70°$ represents the emission of CdTe NCs in the opal without influence of the directional PBG [Fig. 1(c)], i.e., characterizes electronic transitions in the CdTe-opal composite. The anisotropy of PL spectra is clearly seen from comparison of PL spectra collected at $\theta=0°$ and 30°. Transmission spectra of the bare opal and the CdTe-opal show dips centered at 2.23 and

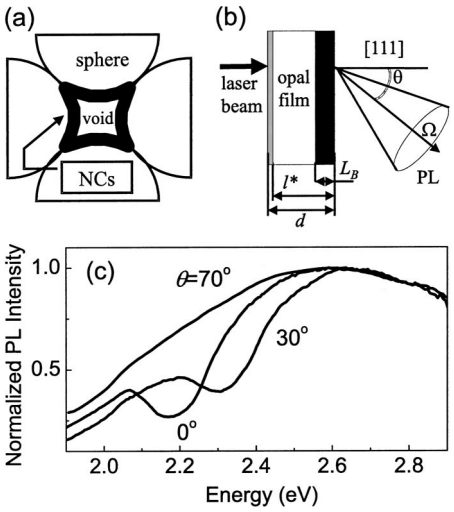

FIG. 1. (a) Schematics of CdTe NCs positioning in octahedral voids of the opal. (b) Experiment layout: d, film thickness; l^*, MFP; L_B, the Bragg attenuation length; θ, angle of detection; Ω, solid angle of emission collection. (c) Normalized angular-resolved PL spectra of a CdTe-loaded opal at different angles of the light collection.

2.18 eV, respectively. The dip midfrequency $\hbar\omega_B = 2\pi c/[2n_{av}(0.816D)]$ corresponds to the Bragg resonance at (111) planes of the fcc lattice, where n_{av} is the average RI obtained from the effective medium approximation and c is the speed of light in vacuum. From the "redshift" of the gap central frequency in CdTe opal (Fig. 2), the fraction of CdTe can be estimated as 1–2 vol. %. Another effect of CdTe impregnation is the reduced transmission above the absorption band edge of NCs. The relative bandwidth of the transmission minimum $\Delta E/E_B \approx 0.067$ exceeds by 20% the gap width calculated for bare opal [17], which indicates a good ordering of thin film opals comparing to bulk opals with characteristic fourfold to sixfold broadening [18].

The PL dip is centered at the same frequency as the transmission minimum and shows 60% intensity reduction. The reasons for a shallow emission dip are the diffuse scattering of the emitted radiation and the near-surface emission. The latter comes from the volume with the transverse dimension below the Bragg attenuation length L_B [Fig. 1(b)]. In the CdTe-opal film $L_B \approx 2$ μm, deduced from the Bragg peak width $\Delta E/E_B \approx 2d/\pi L_B$, where $d = 0.816D$ is the spacing of (111) planes. The diffuse background is comprised by photons scattered at lattice defects. In thin film opals the MFP is about 15 μm [Fig. 1(b)], i.e., no effective scrambling of photon trajectories is expected if detection is along the film normal. Consequently, the less pronounced dip at larger angles of detection is a result of a longer light path.

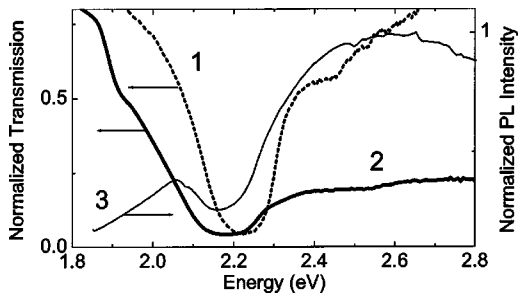

FIG. 2. Transmission spectra of bare (1) and CdTe opal (2) for $\theta = 0°$. PL spectrum of CdTe opal at the same angle (3).

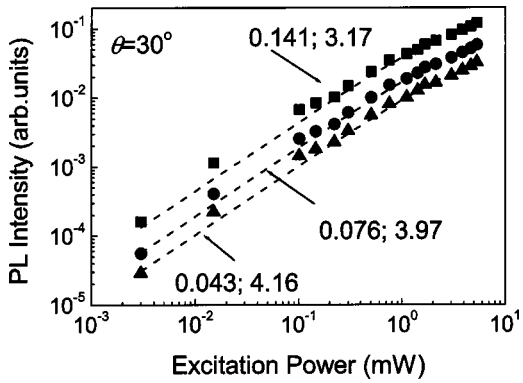

FIG. 3. PL intensity against excitation power recorded at $\theta = 30°$ for $\hbar\omega = 2.5$, 2.3, and 2 eV represented by squares, circles, and triangles, respectively. Lines show two-parameter fits of these input-output characteristics. Fit parameters are shown at curves.

The PL intensity as a function of the excitation power can be represented by input-output characteristics (Fig. 3). These characteristics exhibit saturation with increasing excitation power P for all frequencies in the explored range and are thus fitted to the expression $I_{PL} = I_0[1 - \exp(-P/P_0)]$. The prefactor I_0 is the power radiated at a given frequency by a saturated emitter and the parameter P_0 is the emission saturation threshold. Parameters can be represented in a spectral form. The $I_0(\hbar\omega)$ spectrum at $\theta = 70°$ is a monotonous function of frequency (Fig. 4). It is measured in intensity units and closely resembles the PL spectrum. The parameter $P_0(\hbar\omega)$ is given in power units and corresponds to the projected excitation leading to a complete saturation of the input-output curve.

The $I_0(\hbar\omega)$ spectra at $\theta = 0°$ and 30° follow the canvas for the 70° direction with the exception of the clearly resolved minimum superimposed on the monotonous background (Fig. 4). Moreover, $I_0(\hbar\omega)$ spectra closely resemble the PL spectra including the PBG dip. By contrast, the $P_0(\hbar\omega)$ spectra at $\theta = 0°$ and 30° have their maxima in the PBG. In particular, $P_0(\hbar\omega)$ maximum is centered at the low frequency edge of the PBG, it spreads over the whole PBG range and follows the PBG angular dispersion. The $P_0(\hbar\omega)$ magnitude is nearly doubled in the gap along the [111] axis, but its resolution becomes worse with increasing detection angle.

The similar positions of NCs with respect to the EM field distribution in the unit cell of the opal let us assume that the coupling strength for all emitters radiating in one and the same optical mode is nearly identical. In the case of a saturated emitter and in the presence of an effective nonradiative recombination channel, the radiated power is proportional to the spontaneous emission (SE) rate in a given mode. The PL spectrum collected along a given direction is an estimate of the SE power, if the ballistic regime is preserved. Correspondingly, the smaller the solid angle of emission collection, the better is the approximation of the SE rate in a se-

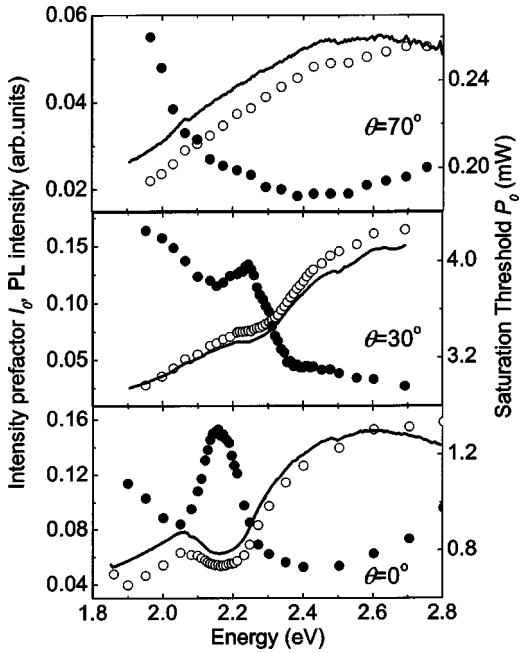

FIG. 4. Parameter spectra at $\theta=70°$, 30°, and 0°. I_0 and P_0 denoted by open and closed circles, respectively. PL spectra (lines) are shown for comparison.

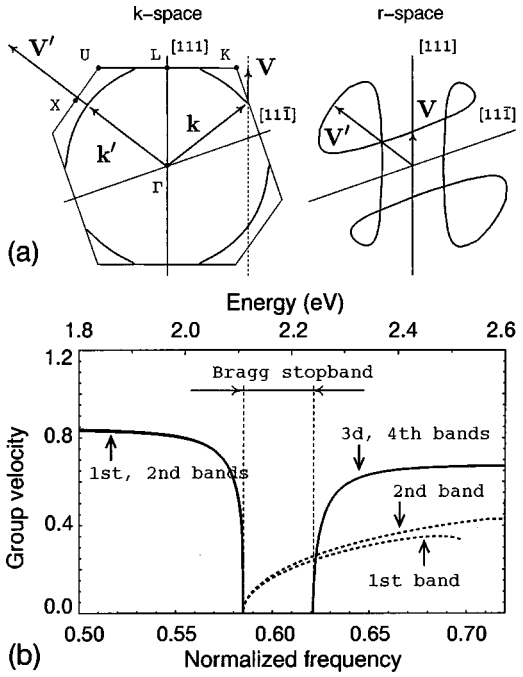

FIG. 5. (a) Isoenergy and group velocity contours of opal for a frequency within the Bragg PBG. $\mathbf{k}'(\mathbf{k})$ and $\mathbf{V}'(\mathbf{V})$ are the wave vector and the group velocity of type 1 (2) mode. (b) Group velocities of type 1 (solid curves) and type 2 (dash curves) Bloch modes along the [111] direction. The group velocity is given in units of the speed of light in vacuum.

lected mode by the $I_0(\hbar\omega,\theta)$ spectrum. The good correlation between $I_0(\hbar\omega)$ and the PL spectrum (Fig. 4) suggests that the SE dominates the radiative relaxation of NCs.

For a given number of NCs, the saturation threshold depends on (i) the population of electron bands in NCs, (ii) the coupling of the emitted photon to the optical modes of the PhC, and (iii) the balance between radiative and nonradiative relaxation. In our opinion, the shape of the $P_0(\hbar\omega)$ spectrum at $\theta=70°$ is dominated by processes in the electronic system of the CdTe NCs [factor (i)]. Assuming the same excitation conditions for all detection angles, the saturation threshold depends on the interplay of factors (ii) and (iii). Thus the increase of the saturation threshold results from faster radiation relaxation or emission stimulation.

The acceleration of the emission rate is a consequence of resonant conditions applied to the emitter. An example of a resonator inside the opal is a lattice defect with eigenmodes matching the Bragg cone. The quality factor of defect modes depends on the distance from the opal boundary, the detuning of the resonant frequency from the PBG center, and on coupling to similar defects. The radiation coupled to the defect eigenmode is localized in the defect vicinity. Consequently, the radiated power acquires a nonlinear component due to the back reaction of the emitted radiation upon the radiative transition probability. In the directional PBG, this effect also acquires the related anisotropy. In an opal, the defect modes are coupled throughout the film and the resulting quality factor is low. However, this model cannot explain the systematic shift of the maximum in $P_0(\hbar\omega)$ towards the low frequency edge.

Another resonance conditions arise due to slowly propagating modes [15]. Anisotropy of PhC gives rise to beam steering effects [19]. As a result, the actual direction of the energy flow inside a PhC does not necessarily coincide with the mode wave vector $\mathbf{k}$. The isoenergy surface of an opal in k space in the PBG range contains eight necks, two per each [111] axis [Fig. 5(a)] [20]. When this surface crosses the boundary of the first Brillouin zone (FBZ), the normal component of the group velocity vector $\mathbf{V}$ vanishes. This means that all eigenmodes, the wave vectors of which end up at the intersection of the neck with the zone boundary, have the group velocity pointing along the FBZ boundary. Some eigenmodes with wave vectors near the [11$\bar{1}$] direction and group velocity pointing in the [111] direction are expected [Fig. 5(a)]. Because the direction of energy transport in a nonabsorbing PhC coincides with the group velocity direction [19], there should always be some energy flux in the Bragg cone. In what follows, we will refer to modes with wave vectors parallel to the group velocity vector as type 1 modes and to other modes as type 2 modes.

Figure 5(b) shows the calculated group velocities along the [111] axis for wave vectors of the XULK section of the opal FBZ. Calculations were performed using the plane wave expansion method [22]. The best fit to experimental data was obtained for $D=243$ nm and refractive index $n=1.6$. It is instructive to separate contributions to the energy flux along the [111] direction from type 1 and type 2 eigenmodes. For frequencies below the Bragg PBG, the flux is solely formed by type 1 modes of the first and second photonic bands. Within the PBG, only type 2 modes of the first and second bands contribute to the flux. Above the PBG, the flux is composed by the type 2 modes of the first and second bands as well as by the type 1 and type 2 modes of the third and

fourth bands. For sake of clarity, contributions of the latter are omitted in Fig. 5(b), because their frequencies are above the Bragg PBG.

The group velocity vanishes at the low frequency PBG edge in the ballistic limit of an infinite PhC and then grows slowly with increasing frequency, comprising, in average, 1/10 of the group velocity outside the PBG. Correspondingly, within the PBG type 2 modes traverse the opal slowly and interact with the pumped medium for longer time. Zero group velocity at the low frequency PBG edge is the reason for the "redshift" of the $P_0(\hbar\omega)$ spectrum maximum with respect to the PBG center (Fig. 4). The relative number of type 2 modes is proportional to the ratio of the small solid angle in k space, $d\Omega_k$, and the corresponding solid angle in real space, $d\Omega$, and is given by $N \sim \Sigma d\Omega_k / d\Omega$, where the summation is taken over all contributions to the energy flux [20]. Since the type 2 modes originate at the necks of the isoenergy surface, the ratio is small all over the PBG (<5 %) [Fig. 5(a)]. Correspondingly, the contribution of the stimulated emission to the total PL signal is small.

When approaching the PhC boundary, type 2 modes should experience refraction. According to the Snell law, a mode with the group velocity pointing along [111] direction inside the opal should deviate from this direction outside the opal [Fig. 5(a)]. However, the Snell law is not valid for type 2 modes due to their strongly inhomogeneous nature. An analysis of the inhomogeneous Bloch wave refraction at the PhC-air interface should include all spatial harmonics constituting the mode. Rigorous finite difference time domain (FDTD) calculations show that the refracted inhomogeneous type 2 modes keep their propagation direction outside the crystal [21].

In summary, the emission intensity of CdTe opal was studied as a function of the excitation power over a wide energy range including the directional PBG. The essential differences with previously studied opal-based materials are (i) the close to ballistic regime of the emission propagation, which avoids averaging over all emission directions, and (ii) the position of the emitter in accord with the EM field pattern in the opal unit cell, which avoids averaging of the coupling strength between emitter and optical modes. A two-parameter fitting of saturating input-output characteristics reveals the increase of the saturation threshold in the PBG. This observation was interpreted in terms of the stimulation of the emission by the EM field of resonating eigenmodes of the PBG range. The modeling of resonance conditions was based on slow and strongly inhomogeneous modes.

This research was supported by the DFG Priority Program "Photonic Crystals" and EU Project No. IST 1999-19009 PHOBOS.

[1] V. P. Bykov, Sov. Phys. JETP **35**, 269 (1972).
[2] E. Yablonovitch, Phys. Rev. Lett. **58**, 2059 (1987).
[3] S. John and J. Wang, Phys. Rev. Lett. **64**, 2418 (1990).
[4] E. Yablonovitch, J. Mod. Opt. **41**, 173 (1994).
[5] M. N. Shkunov *et al.*, Adv. Funct. Mater. **12**, 21 (2002).
[6] A. F. Koenderink *et al.*, Phys. Rev. Lett. **88**, 143903 (2002).
[7] Y. Xia *et al.*, J. Adv. Mater. **12**, 693 (2000).
[8] S. G. Romanov and C. M. Sotomayor Torres (unpublished).
[9] E. P. Petrov *et al.*, Phys. Rev. Lett. **81**, 77 (1998).
[10] M. Megens *et al.*, Phys. Rev. A **59**, 4727 (1999).
[11] Yu. A. Vlasov *et al.*, Appl. Phys. Lett. **71**, 1616 (1998).
[12] X.-H. Wang *et al.*, Phys. Rev. Lett. **88**, 093902 (2002).
[13] A. L. Rogach, Mater. Sci. Eng., B **69**, 435 (2000).
[14] K. Busch *et al.*, Phys. Rev. E **62**, 4251 (2000).
[15] K. Sakoda, Opt. Express **4**, 167 (1998).
[16] N. Gaponik *et al.*, J. Phys. Chem. B **106**, 7177 (2002).
[17] S. G. Romanov *et al.*, Phys. Rev. E **63**, 056603 (2001).
[18] V. N. Astratov *et al.*, Phys. Rev. B **66**, 165215 (2002).
[19] P. Yeh, *Optical Waves in Layered Media* (Wiley, New York, 1998); P. St. J. Russell, Appl. Phys. B: Photophys. Laser Chem. **39**, 231 (1986); H. Kosaka *et al.*, Phys. Rev. B **58**, R10096 (1998).
[20] D. N. Chigrin *et al.* (unpublished).
[21] D. N. Chigrin (unpublished).
[22] S. G. Johnson and J. D. Joannopoulos, Opt. Express **8**, 173 (2001).